



HAL
open science

Uniaxial stress effect on the $1A_1 \rightarrow 1T_1$ transition of Co^{3+} in $\alpha-Al_2O_3$

E. Duval, R. Louat, Bernard Champagnon, R. Lacroix, J. Weber

► **To cite this version:**

E. Duval, R. Louat, Bernard Champagnon, R. Lacroix, J. Weber. Uniaxial stress effect on the $1A_1 \rightarrow 1T_1$ transition of Co^{3+} in $\alpha-Al_2O_3$. *Journal de Physique*, 1975, 36 (6), pp.559-569. 10.1051/jphys:01975003606055900 . jpa-00208287

HAL Id: jpa-00208287

<https://hal.science/jpa-00208287>

Submitted on 4 Feb 2008

HAL is a multi-disciplinary open access archive for the deposit and dissemination of scientific research documents, whether they are published or not. The documents may come from teaching and research institutions in France or abroad, or from public or private research centers.

L'archive ouverte pluridisciplinaire **HAL**, est destinée au dépôt et à la diffusion de documents scientifiques de niveau recherche, publiés ou non, émanant des établissements d'enseignement et de recherche français ou étrangers, des laboratoires publics ou privés.

Classification
 Physics Abstracts
 8.830

UNIAXIAL STRESS EFFECT ON THE ${}^1A_1 \rightarrow {}^1T_1$ TRANSITION OF Co^{3+} IN $\alpha\text{-Al}_2\text{O}_3$

E. DUVAL, R. LOUAT, B. CHAMPAGNON

Laboratoire de Spectroscopie et de Luminescence
 Université Claude-Bernard, 69621 Villeurbanne, France

R. LACROIX, J. WEBER

Département de Chimie Physique, Université de Genève, Suisse

(Reçu le 29 janvier 1975, accepté le 21 février 1975)

Résumé. — L'effet d'une contrainte uniaxiale sur les raies d'absorption de plus basse énergie de la transition ${}^1A_1 \rightarrow {}^1T_1$ de Co^{3+} dans $\alpha\text{-Al}_2\text{O}_3$ est étudié. Les spectres sous contrainte sont interprétés par une matrice phénoménologique basée sur la théorie des groupes. Des informations sont obtenues sur la déformation locale et l'interaction ion-déformation à partir des paramètres expérimentaux mesurés sur les spectres. Les valeurs relatives des constantes d'élasticité locales telles que $S_{11}^* - S_{12}^*$, S_{44}^* , S_{14}^* , S_{15}^* , peuvent être déterminées. Les résultats expérimentaux confirment que l'effet Jahn-Teller n'est pas très fort. Les coordonnées normales des modes de vibration responsables de l'effet Jahn-Teller seraient une combinaison linéaire des coordonnées tétraogonales et trigonales.

Abstract. — The effect of uniaxial stress on the lowest energy lines of ${}^1A_1 \rightarrow {}^1T_1$ transition of Co^{3+} in $\alpha\text{-Al}_2\text{O}_3$ is studied. The stress spectra are interpreted by a phenomenological matrix based on group theory. From the experimental parameters measured from the spectra, information is obtained on the local deformation and ion-strain interaction. The relative values of local elastic compliances such as $S_{11}^* - S_{12}^*$, S_{44}^* , S_{14}^* , S_{15}^* can be determined. The experimental constants which depend on the ion-strain coupling confirm that the Jahn-Teller effect is not very strong. The normal coordinates of the vibration modes responsible of the Jahn-Teller effect are found to be a linear combination of tetragonal and trigonal coordinates.

1. **Introduction.** — The effect of an uniaxial stress on the transition between a fundamental singlet state and the three lower vibronic states proceeding from a T_1 or T_2 state in cubic symmetry of $(3d)^n$ ions in $\alpha\text{-Al}_2\text{O}_3$ has been theoretically studied in paper-2 [1]. With these ions we always observed a Jahn-Teller effect. When it is very strong, the eigenfunctions for the three lower vibronic excited states are ψ_1, ψ_2, ψ_3 if an uniaxial stress transforming as the basis functions of the E -representation of the C_{3v} group is applied. These functions correspond to the relaxed states in each of the three potential wells created by the Jahn-Teller coupling with vibration E -modes. When the Jahn-Teller coupling is not very strong the basis vibronic wave-functions are χ_1, χ_2, χ_3 . The χ_1, χ_2 functions transform as the basis functions of the E -representation of the C_{3v} group, χ_3 as the A_1 or A_2 basis functions. In the case of the ${}^4A_2 \rightarrow {}^4T_2$ zero-phonon transition of Cr^{3+} , the Jahn-Teller effect is strong and the good eigenfunctions are ψ_1, ψ_2, ψ_3 as it has been shown in paper-1 [2] and paper-3 [3].

In this paper we study the effect of the uniaxial stress on the lowest energy vibronic transition between the 1A_1 and 1T_1 levels of the Co^{3+} ion in $\alpha\text{-Al}_2\text{O}_3$. The pressure has been applied successively along the five directions chosen for Cr^{3+} . This transition appears as a strong absorption line in polarization perpendicular to the trigonal C_3 -axis, and as a weak line in polarization parallel to the C_3 -axis, shifted towards the high energy from the first line by about 61 cm^{-1} . The strong line is allowed and the weak line forbidden in C_{3v} symmetry. Such a splitting does not appear in the ${}^4A_2 \rightarrow {}^4T_2$ zero-phonon transition of Cr^{3+} . Taking into account the relative strong intensity of the lowest vibronic transition between the 1A_1 and 1T_1 levels, and the splitting of about 61 cm^{-1} , we believe that the Jahn-Teller effect is not so strong in the 1T_1 state of Co^{3+} as in the 4T_2 state of Cr^{3+} . Actually the strong line corresponds to the transition from the singlet 1A_1 to the doublet χ_1, χ_2 and the weak line to the transition from 1A_1 to the singlet χ_3 . An uniaxial stress will mix the vibronic states χ_1, χ_2, χ_3 . The effect of an

uniaxial stress on the spectrum is interpreted by the phenomenological matrix in the χ -representation given in the paper-2. We can now from the stress spectra, estimate the relative values of local elastic compliances such as $S_{11}^* - S_{12}^*$, S_{44}^* , S_{15}^* , S_{14}^* . We also deduce the ratio of the ion-strain interaction constants with the E -strains. From this last experimental result we try to obtain information about the modes responsible of the Jahn-Teller effect. A comparison with the results obtained for Cr^{3+} is given.

2. Experimental results. — The absorption spectra have been obtained with an Hilger-Ebert scanning monochromator, having a 4 Å/mm dispersion in the first order. In order to realise good signal/noise ratios, particularly for the weak lines, the modulated polarization technique was used [4]. Most of the spectra have been obtained at 77 K.

The single crystals ⁽¹⁾ were oriented from X-ray diffraction diagrams. The orientation was precise as a result of the use of a polarizing microscope. The relative mass concentration of Co^{3+} was 10^{-4} .

2.1 ABSORPTION SPECTRA WITHOUT STRESS. — At low temperature when the light is polarized $E \perp C_3$, a strong absorption line appears at 6 878 Å ($14\,535\text{ cm}^{-1}$) accompanied by a vibrational structure whose frequencies appear to be the same as the corundum frequencies [5]. Towards higher energies, at $61.5 \pm 1.5\text{ cm}^{-1}$ from this line, there is a weaker line, polarized $E // C_3$, the intensity ratio being approximately 15. The weak line at $14\,553\text{ cm}^{-1}$

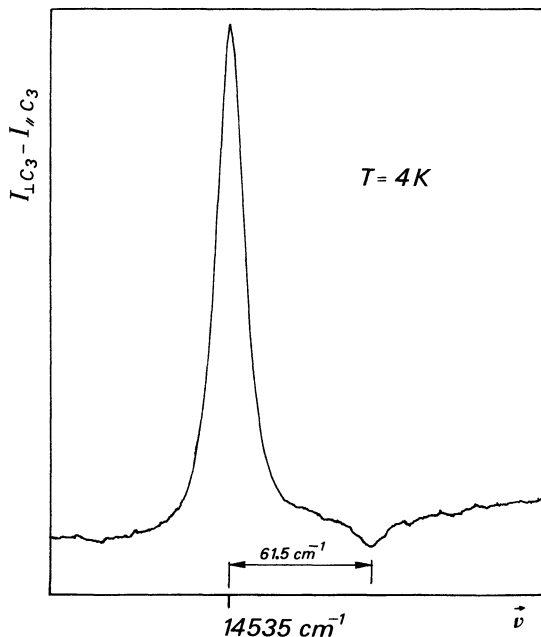


FIG. 1. — Linear dichroism of the ${}^1A_1 \rightarrow {}^1T_1$ lowest energy lines in the free crystal.

⁽¹⁾ Crystals purchased from « Centre de Recherches Ugine-Kuhlman » 38-Jarrie, France.

observed by D. S. McClure [5] in $E // C_3$ polarization does not appear in our spectra even after numerous scans averaged by memory stores. In figure 1 we show the spectrum for these two transitions obtained by the modulation of polarization. For the trigonal splitting measured on the absorption bands, McClure gives a value equal to 360 cm^{-1} . Now, the strong line ($E \perp C_3$) corresponds to the transition from the 1A_1 fundamental state to the lowest energy degenerated vibronic states χ_1 and χ_2 of the 1T_1 level, and the weaker line ($E // C_3$) to the transition between the A_1 and χ_3 states, which is allowed in C_3 symmetry. Thus, it appears that the splittings between the vibronic states χ_1 , χ_2 and χ_3 and between the E_+ , E_- , A_2 electronic states are quite different, since the splitting measured on the bands is not altered by the lattice vibrations, as shown by C. H. Henry *et al.* [6].

2.2 EFFECT OF A PRESSURE APPLIED ALONG THE C_3 -AXIS. — Such a stress does not alter the trigonal symmetry of the Co^{3+} site. The two lines shift linearly towards higher energies when the pressure increases. The shift of the line polarized $E \perp C_3$ is a little larger than the shift of the line polarized $E // C_3$ (Fig. 2).

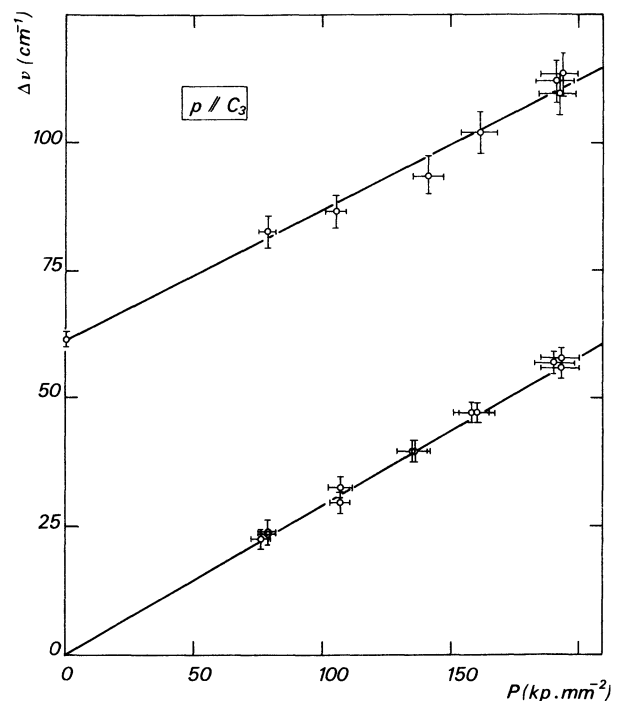


FIG. 2. — Shifts of the ${}^1A_1 \rightarrow {}^1T_1$ lowest energy lines as a function of the applied pressure parallel to the C_3 -axis.

2.3 EFFECT OF A PRESSURE APPLIED ALONG AN AXIS PERPENDICULAR OR PARALLEL TO A C_2 AXIS AND PERPENDICULAR TO THE C_3 -AXIS. — Under the effect of such a stress, the site symmetry becomes C_1 if one proceeds from C_3 . Thus, the degeneracy of the vibronic state is removed. We observed effectively the splitting of the strong line ($E \perp C_3$) into two components. From 120 kp.mm^{-2} the mixing of the vibronic states χ_1 , χ_2 with χ_3 becomes visible : the third line

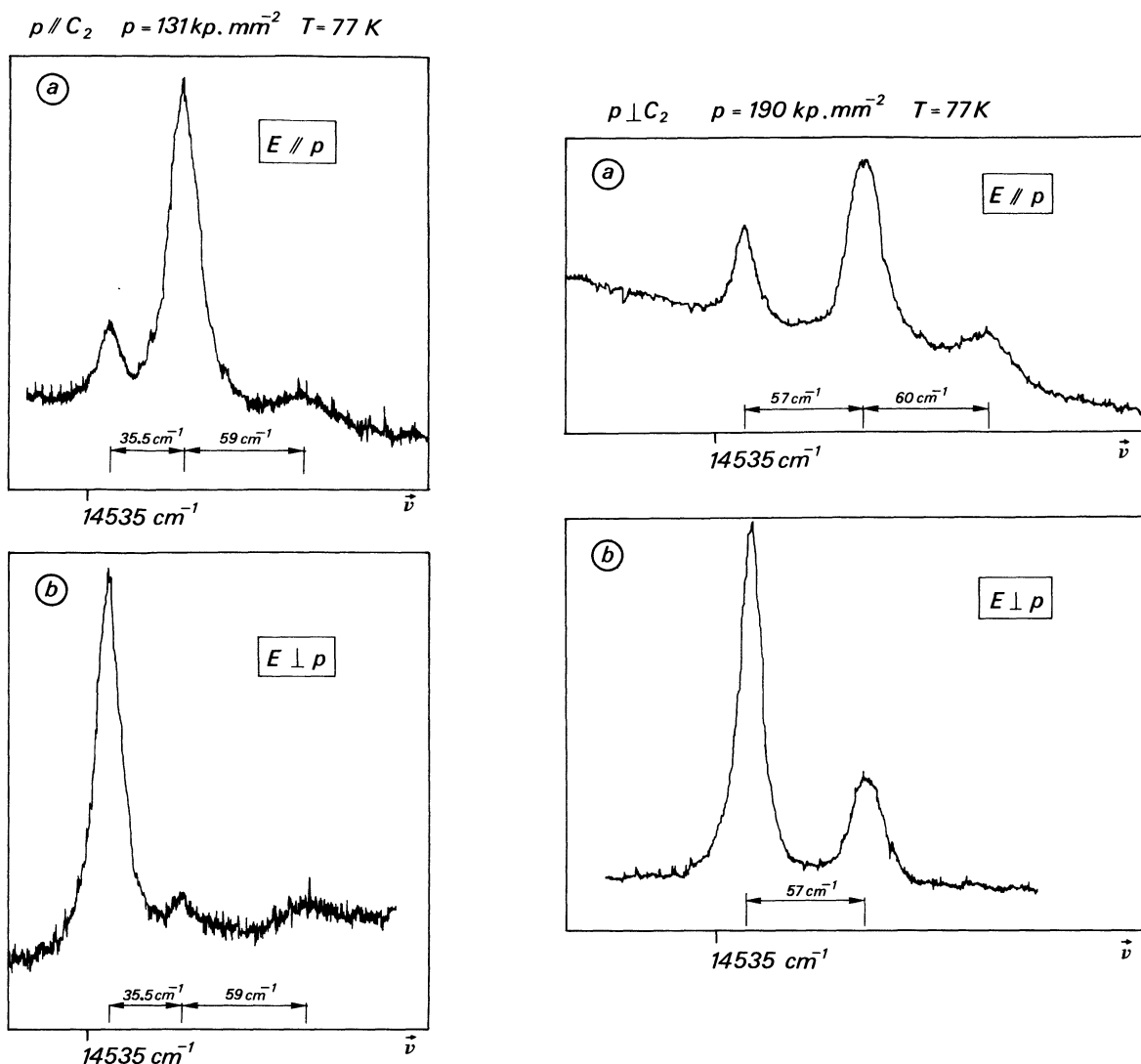


FIG. 3. — Spectra of the ${}^1A_1 \rightarrow {}^1T_1$ lowest energy lines for an applied pressure perpendicular to the C_3 axis and parallel or perpendicular to the C_2 axis.

which was polarized $E // C_3$ appears in polarization $E \perp C_3$, and the two strong lines at lower energies are repulsed by the third one (Fig. 3 and Fig. 4).

2.4 EFFECT OF A PRESSURE APPLIED ALONG AN AXIS WHOSE DIRECTION COSINES ⁽²⁾ ARE $k = \pm 0.90, l = 0, m = 0.44$. — The direction of this pressure lies in the plane xz and makes an angle of $\theta = 26^\circ$ with Ox , so that the crystal is submitted in particular to a σ_{xz} stress. The direction of this stress is opposite for the sites of II-type and the sites of III-type [1]. Therefore, under this pressure the strong line is split into four lines, two lines belonging to the sites of II-type and the two others to the sites of III-type.

⁽²⁾ The direction cosines are relative to the x, y, z coordinate axes of the cation site [2]. Ox is parallel to the twofold C_2 -axis of the crystal and Oz is parallel to the three-fold C_3 -axis.

The weak line polarized $E // C_3$ does not appear split, because the line is wide and the splitting small. The maximum pressure was limited to $68 \text{ kp} \cdot \text{mm}^{-2}$ because the crystal is fragile for this direction of pressure. (Fig. 5 and Fig. 6)

2.5 EFFECT OF A PRESSURE APPLIED ALONG AN AXIS WHOSE DIRECTION COSINES ARE $k = 0, l = 0.906, m = 0.423$. — The direction of this pressure lies in the plane yz and makes an angle of $\theta = 25^\circ$ with Oy . The direction of the σ_{yz} stress is the same for any site. Thus, the strong line is split into two lines. The splitting between these two lines is about twice that obtained for a pressure applied along an axis perpendicular or parallel to a C_2 -axis and perpendicular to the C_3 -axis. We have limited the pressure to $100 \text{ kp} \cdot \text{mm}^{-2}$, because the crystal is fragile, although less than for the previous direction of pressure. (Fig. 7)

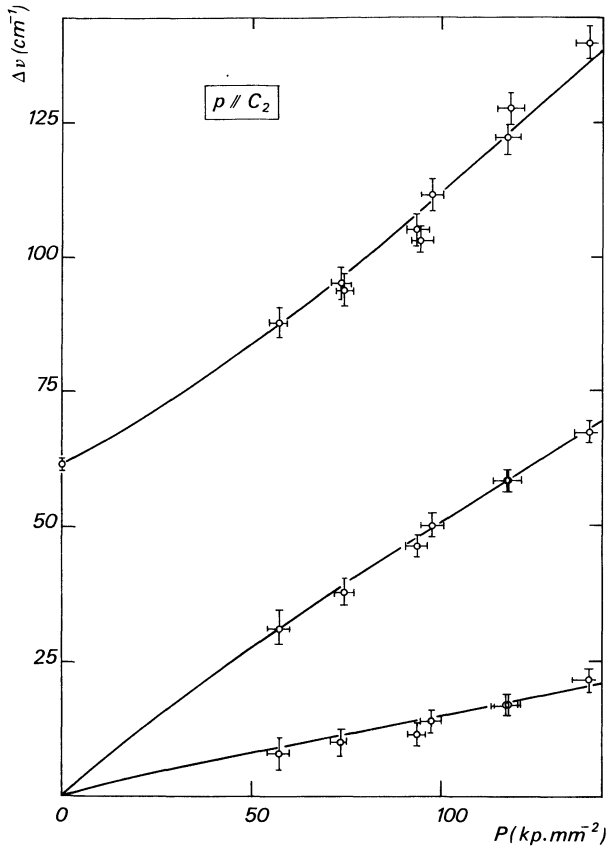


FIG. 4a. — Shifts of the split components of the ${}^1A_1 \rightarrow {}^1T_1$ lowest energy lines as a function of the applied pressure parallel to C_2 -axis.

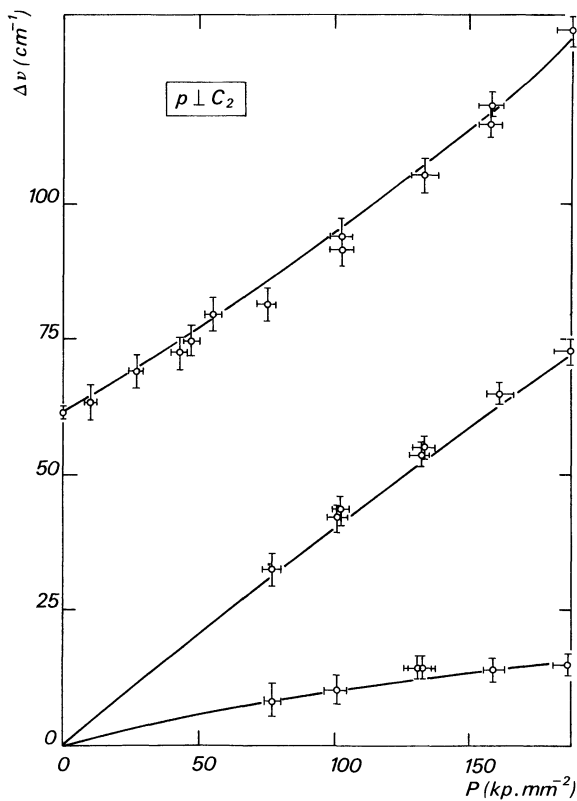


FIG. 4b. — Shifts of the split components of the ${}^1A_1 \rightarrow {}^1T_1$ lowest energy lines as a function of the applied pressure perpendicular to the C_3 and C_2 axes. The solid lines are calculated from the experimental parameters.

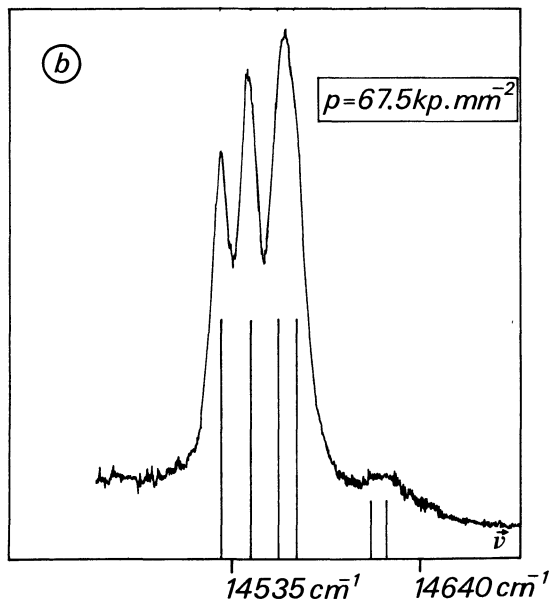
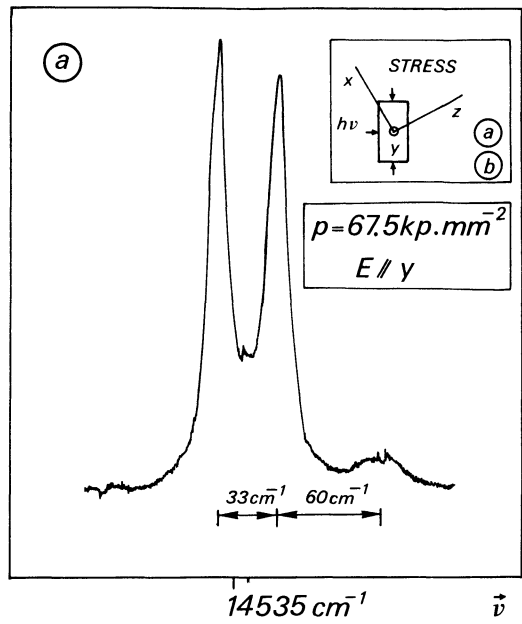


FIG. 5. — Spectra of the ${}^1A_1 \rightarrow {}^1T_1$ lowest energy lines for a pressure applied along an axis whose direction cosines are $k = \pm 0.90$, $l = 0$, $m = 0.44$. The lines positions in no-polarized b -spectrum are compared to the calculated positions.

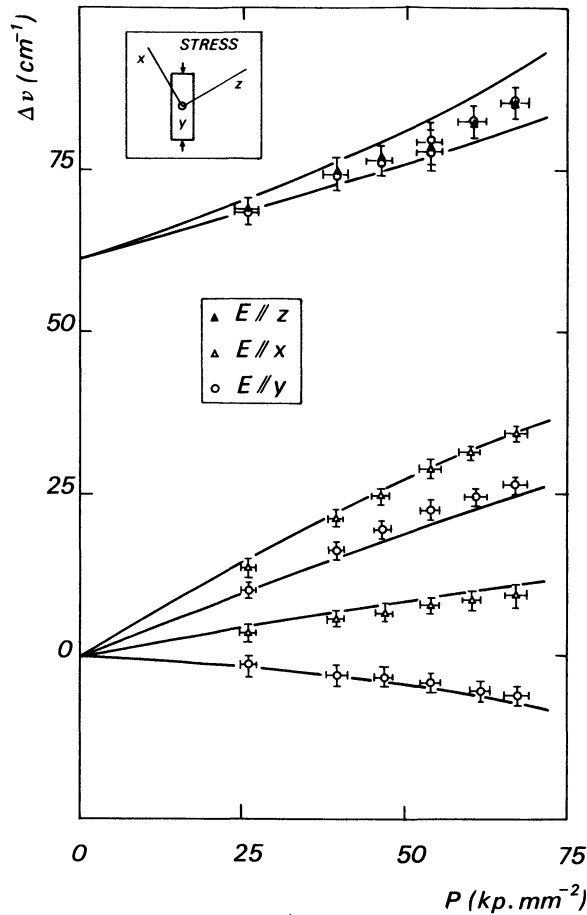


FIG. 6. — Shifts of the split components of the ${}^1A_1 \rightarrow {}^1T_1$ lowest energy lines as a function of the pressure applied along an axis whose direction cosines are $k = \pm 0.90$, $l = 0$, $m = 0.44$. The solid lines are calculated from the experimental parameters.

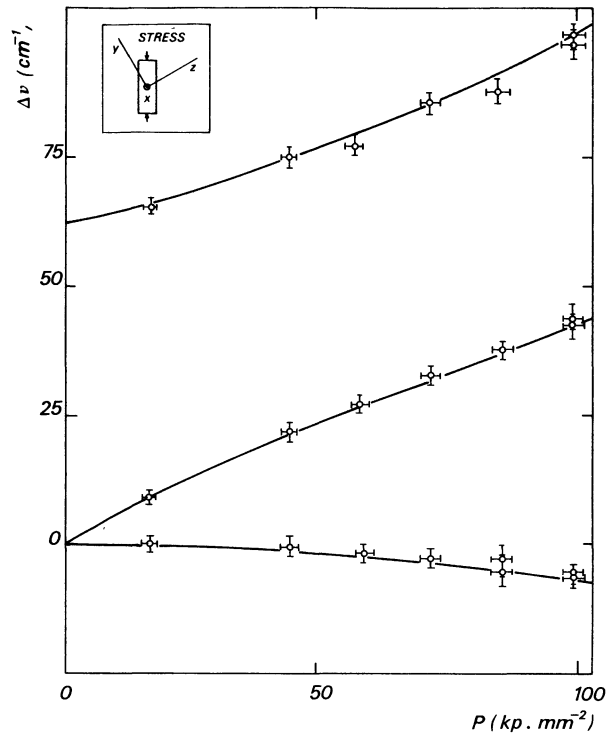


FIG. 7. — Shifts of the split components of the ${}^1A_1 \rightarrow {}^1T_1$ lowest energy lines as a function of the pressure applied along an axis whose direction cosines are $k = 0$, $l = 0.906$, $m = 0.423$. The solid lines are calculated from the experimental parameters.

3. Determination of the experimental parameters. —

The strain hamiltonian has been given in the eq. (8) of the paper-2 [1]. For a pressure p applied along an axis defined by its direction cosines k , l , m relatively to the Ox , Oy , Oz axis of the site II, and k , $-l$, $-m$ relatively to the axes of the site III it is given by :

$$\begin{aligned}
 \mathcal{H}_d = & -p \left\{ V_1 \frac{1}{\sqrt{3}} [(k^2 + l^2) (S_{11}^* + S_{12}^*) + m^2 S_{33}^* + (k^2 + l^2 + 2m^2) S_{13}^*] \right. \\
 & + V_1' \frac{1}{\sqrt{6}} [2m^2 S_{33}^* + 2(k^2 + l^2 - m^2) S_{13}^* - (k^2 + l^2) (S_{11}^* + S_{12}^*)] \\
 & + V_+ \frac{1}{\sqrt{2}} [(k^2 - l^2) (S_{11}^* - S_{12}^*) + 2lmS_{14}^* \pm 2kmS_{15}^*] \\
 & - V_- \sqrt{2} [\pm kl(S_{11}^* - S_{12}^*) \pm kmS_{14}^* - lmS_{15}^*] \\
 & + V_+ \frac{1}{\sqrt{2}} [\pm kmS_{44}^* \pm 2klS_{14}^* + (k^2 - l^2) S_{15}^*] \\
 & \left. + V_- \frac{1}{\sqrt{2}} [(k^2 - l^2) S_{14}^* + lmS_{44}^* \mp 2klS_{15}^*] \right\}. \quad (1)
 \end{aligned}$$

The upper sign corresponds to sites I and II and the lower one to sites III or IV. The S_{ij}^* are the effective local elastic compliances [1].

The shifts and splittings due to uniaxial stress depend on the following experimental parameters t , a'' , b'' , c_1' , c_2' , μ and ν [1] :

$$\begin{aligned}
 \langle \chi_1 | V_1 | \chi_1 \rangle - \langle A_1 | V_1 | A_1 \rangle &= \langle \chi_2 | V_1 | \chi_2 \rangle - \langle A_1 | V_1 | A_1 \rangle = \\
 &= \langle \chi_3 | V_1 | \chi_3 \rangle - \langle A_1 | V_1 | A_1 \rangle = -\frac{t}{\sqrt{3}} \quad (2)
 \end{aligned}$$

$$\begin{aligned} \langle \chi_1 | V_+ | \chi_1 \rangle &= - \langle \chi_2 | V_+ | \chi_2 \rangle = \langle \chi_1 | V_- | \chi_2 \rangle = \frac{b''}{4\sqrt{2}} \\ \langle \chi_1 | V'_+ | \chi_1 \rangle &= - \langle \chi_2 | V'_+ | \chi_2 \rangle = \langle \chi_1 | V'_- | \chi_2 \rangle = \frac{a''}{2\sqrt{2}} \end{aligned} \quad (3)$$

$$\begin{aligned} \langle \chi_1 | V_+ | \chi_3 \rangle &= - \langle \chi_2 | V_- | \chi_3 \rangle = \frac{\mu b''}{4} \\ \langle \chi_1 | V'_+ | \chi_3 \rangle &= - \langle \chi_2 | V'_- | \chi_3 \rangle = \frac{\nu a''}{2} \end{aligned} \quad (4)$$

$$\begin{aligned} \langle \chi_1 | V'_1 | \chi_1 \rangle - \langle A_1 | V'_1 | A_1 \rangle &= \langle \chi_2 | V'_1 | \chi_2 \rangle - \langle A_1 | V'_1 | A_1 \rangle = - \frac{c'_1}{\sqrt{6}} \\ \langle \chi_3 | V'_1 | \chi_3 \rangle - \langle A_1 | V'_1 | A_1 \rangle &= - \frac{c'_2}{\sqrt{6}}. \end{aligned} \quad (5)$$

The operators V_1 and V'_1 do not mix the χ_1, χ_2, χ_3 states. Then, the partial shifts due to the

$$\frac{\varepsilon_{xx}^* + \varepsilon_{yy}^* + \varepsilon_{zz}^*}{3} \quad \text{and} \quad \frac{2\varepsilon_{zz}^* - \varepsilon_{xx}^* - \varepsilon_{yy}^*}{6}$$

strains are, from the eq. (1), (2), (5) :

$$ph_{\parallel}^{(1,2)} = p \left[\frac{t}{3} (S_{33}^* + 2 S_{13}^*) + \frac{c'_1}{3} (S_{33}^* - S_{13}^*) \right] + \langle A_1 | \mathcal{J}C_d | A_1 \rangle \quad (6)$$

for the transitions ${}^1A_1 \rightarrow \chi_1$ or χ_2 , and :

$$ph_{\parallel}^{(3)} = p \left[\frac{t}{3} (S_{33}^* + 2 S_{13}^*) + \frac{c'_2}{3} (S_{33}^* - S_{13}^*) \right] + \langle A_1 | \mathcal{J}C_d | A_1 \rangle \quad (6')$$

for the transition ${}^1A_1 \rightarrow \chi_3$.

When the pressure is perpendicular to the C_3 -axis :

$$ph_{\perp}^{(1,2)} = p \left[\frac{t}{3} (S_{11}^* + S_{12}^* + S_{13}^*) - \frac{c'_1}{6} (S_{11}^* + S_{12}^* - 2 S_{13}^*) \right] + \langle A_1 | \mathcal{J}C_d | A_1 \rangle \quad (7)$$

$$ph_{\perp}^{(3)} = p \left[\frac{t}{3} (S_{11}^* + S_{12}^* + S_{13}^*) - \frac{c'_2}{6} (S_{11}^* + S_{12}^* - 2 S_{13}^*) \right] + \langle A_1 | \mathcal{J}C_d | A_1 \rangle. \quad (7')$$

If the direction cosine, with respect to the C_3 -axis of the direction of pressure, is m , the shifts are :

$$h_{<}^{(1,2)} = m^2 h_{\parallel}^{(1,2)} + (1 - m^2) h_{\perp}^{(1,2)} \quad (8)$$

$$h_{<}^{(3)} = m^2 h_{\parallel}^{(3)} + (1 - m^2) h_{\perp}^{(3)}. \quad (8')$$

The parameters $h_{\parallel}^{(1,2)}, h_{\parallel}^{(3)}$ are obtained from figure 2. We find :

$$h_{\parallel}^{(3)} - \frac{1}{p} \langle A_1 | \mathcal{J}C_d | A_1 \rangle = 0.255 \pm 0.025 \text{ cm}^{-1} \text{ kp}^{-1} \text{ mm}^2$$

$$h_{\parallel}^{(1,2)} - \frac{1}{p} \langle A_1 | \mathcal{J}C_d | A_1 \rangle = 0.295 \pm 0.015 \text{ cm}^{-1} \text{ kp}^{-1} \text{ mm}^2$$

The $h_{\perp}^{(3)}, h_{\perp}^{(1,2)}$ parameters are determined from the curve slopes for $p = 0$ on the diagrams of figure 4.

$$h_{\perp}^{(3)} - \frac{1}{p} \langle A_1 | \mathcal{J}C_d | A_1 \rangle = 0.290 \pm 0.01 \text{ cm}^{-1} \text{ kp}^{-1} \text{ mm}^2$$

$$h_{\perp}^{(1,2)} - \frac{1}{p} \langle A_1 | \mathcal{J}C_d | A_1 \rangle = 0.270 \pm 0.01 \text{ cm}^{-1} \text{ kp}^{-1} \text{ mm}^2.$$

For Cr^{3+} in $\alpha-Al_2O_3$ (paper-3) we have shown the equality of the linear compressibilities :

$$S_{33}^* + 2 S_{13}^* = S_{11}^* + S_{12}^* + S_{13}^* .$$

We can assume that this equality subsists for Co^{3+} . We find from the eq. (6), (6'), (7), (7') :

$$\begin{aligned} t(S_{33}^* + 2 S_{13}^*) &= 0.835 \pm 0.04 \text{ cm}^{-1} \text{ kp}^{-1} \text{ mm}^2 \\ c'_1(S_{33}^* - S_{13}^*) &= - 0.07 \pm 0.07 \text{ cm}^{-1} \text{ kp}^{-1} \text{ mm}^2 \\ c'_2(S_{33}^* - S_{13}^*) &= 0.05 \pm 0.05 \text{ cm}^{-1} \text{ kp}^{-1} \text{ mm}^2 . \end{aligned}$$

We use the relations (8) and (8') for determining $h_{\leq}^{(3)}$ and $h_{\leq}^{(1,2)}$ because the determination of curve slopes for $p = 0$ on the diagrams of figures 6 and 7 is rather critical.

The effect of the strain components transforming as the basis functions of the E -representation of the C_{3v} group can be measured now, for the shifts due to the strain components transforming as the A_1 basis functions are known. This effect is interpreted by the phenomenological matrix in the basis of the functions χ_3, χ_+, χ_- , such that

$$\chi_+ = q\chi_1 + r\chi_2, \quad \chi_- = r\chi_1 - q\chi_2$$

(paper-2) :

$$\begin{pmatrix} 2 & dg & fg \\ dg & -1+g & 0 \\ fg & 0 & -1-g \end{pmatrix} . \quad (9)$$

The matrices in the χ_3, χ_2, χ_1 basis are given in the paper-2 in function of the a'', b'', μ, ν parameters and the S_{ij}^* local elastic compliances. They are written again in the appendix.

The elements of this subdiagonalized matrix are function of the experimental parameters g, d, f determined from the shifts and splittings of the lines. These parameters g, d, f are given in table I.

TABLE I

	g (kp/mm ²) ⁻¹	d	f
$k = 1, l = 0, m = 0$	0.71×10^{-2}	∓ 0.95	0.65
$k = 0, l = 1, m = 0$	$- 0.71 \times 10^{-2}$	∓ 0.95	0.65
$k = 0, l = 0.906, m = 0.423$	1.26×10^{-2}	∓ 0.74	0.77

The eigenfunctions of the phenomenological matrix (4) is expressed in the following form :

$$u\chi_+ + v\chi_- + w\chi_3$$

χ_+ and χ_- being the basis functions corresponding to the phenomenological matrix (4).

As it has been shown in paper-2, it will be possible to know the experimental parameters such $\mu, \nu, b''/a''$ and the ratios of the local elastic compliances if we determine the mixing of χ_1 and χ_2 in χ_+ or χ_- , which is measured by the ratio $X = - r/q$. This ratio can be determined by the transition intensities.

The intensity of a transition when the light is polarized $x(E // C_2)$ or $y(E // C_2)$ is :

$$\begin{aligned} I_x &\propto | \langle A_1 | x | u\chi_+ + v\chi_- \rangle |^2 \\ I_y &\propto | \langle A_1 | y | u\chi_+ + v\chi_- \rangle |^2 . \end{aligned} \quad (10)$$

Let us note :

$$\begin{aligned} \langle A_1 | x | \chi_2 \rangle &= \langle A_1 | y | \chi_1 \rangle = - P \\ \langle A_1 | x | \chi_1 \rangle &= - \langle A_1 | y | \chi_2 \rangle = - \pi . \end{aligned}$$

The identities between elements come from Wigner-Eckart's theorem taking into account the time reversal invariance.

We have two types of sites for which the π/P ratio has opposite signs. As we measure the total intensity, the terms in πP of both types of site cancel each other. Thus, the experimental intensities are :

$$\begin{aligned} \langle I_x \rangle &\propto P^2(ur - vq)^2 + \pi^2(uq + vr)^2 \\ \langle I_y \rangle &\propto P^2(uq + vr)^2 + \pi^2(ur - vq)^2 . \end{aligned}$$

From the measurements we obtain only the size of d and f for each of the matrices. Their relative sign remains unknown. It results that the sign of X is unknown and consequently those of a'', S_{15}^* and S_{14}^* . On the other hand the relative sign of $a'' S_{15}^*$ is known. The best fit between experimental and calculated intensities is obtained by the least squares method and corresponds to the values of $X = - r/q$ and π^2/P^2 given in table II.

Now, we know all the elements of matrices $A1$ and $A2$ for the directions of pressure : $k = 1, l = 0, m = 0$ or $k = 0, l = 1, m = 0$ and $k = 0, l = 0.906, m = 0.423$. Resolving the system of equations, we find solutions if $b''(S_{11}^* - S_{12}^*)$ and $a'' S_{15}^*$ have opposite-signs. For Cr^{3+} we found that $b''(S_{11}^* - S_{12}^*)$ and $a' S_{15}^*$ had opposite signs.

The values of the experimental parameters calculated from those of X given in table II, are gathered in

TABLE II

	X	π^2/P^2
$k = 1, l = 0, m = 0$	± 2.56	0.077
$k = 0, l = 1, m = 0$	± 2.56	0.077
$k = 0, l = 0.906, m = 0.423$	± 1.053	0.077

TABLE III

$\frac{ b'' }{ a'' }$	μ	ν	$\frac{S_{44}^*}{S_{11}^* - S_{12}^*}$	$\frac{ S_{14}^* }{S_{11}^* - S_{12}^*}$	$\frac{ S_{15}^* }{S_{11}^* - S_{12}^*}$
2.65	0.70	0.68	2.5	0.14	1.19

the table III. The splittings and shifts obtained with the calculated parameters are compared to the experimental splittings and shifts on the diagrams of figures 4, 6, 7. The limit values of parameters evaluated from the experimental errors are the following :

$$2.5 < \frac{|b''|}{|a''|} < 2.7 \quad 0.68 < \mu < 0.73$$

$$0.65 < \nu < 0.71$$

$$1.5 < \frac{S_{44}^*}{S_{11}^* - S_{12}^*} < 3 \quad 0.12 < \frac{|S_{14}^*|}{S_{11}^* - S_{12}^*} < 0.3$$

$$0.9 < \frac{|S_{15}^*|}{S_{11}^* - S_{12}^*} < 1.3 .$$

From the spectra and these values of parameters we find that the mean value of $b''(S_{11}^* - S_{12}^*)$ is about $5 \text{ cm}^{-1} \cdot \text{kp}^{-1} \cdot \text{mm}^2$.

4. Discussion. — 4.1 LOCAL DEFORMATION. — By these optical measurements we obtain the relative values of the local elastic compliances. Unfortunately it is not possible to know the sign of S_{14}^* and S_{15}^* . The local deformation obeys the C_3 ($\sim C_{3v}$) local symmetry rather than the D_{3d} crystal symmetry. It is somewhat surprising to find $\frac{|S_{15}^*|}{S_{11}^* - S_{12}^*}$ larger than 1. This result is not unreasonable. First of all we measure the deformation by an effect on the ligand field felt by Co^{3+} ion. On the other hand the outside pressure is not applied directly on the cluster around the cation. The stress symmetry which is exerted on the ions of the cluster is modified by the environ-

ment. For Cr^{3+} we have found $\frac{|S_{15}^*|}{S_{11}^* - S_{12}^*} > 0.4$. this result is very consistent with the value of this ratio for Co^{3+} .

4.2 JAHN-TELLER EFFECT. — The experimental results obtained, and especially the splitting observed in the absence of stress, show that the Jahn-Teller effect is not very strong. However we can have a first insight into the problem if the wave functions χ_1, χ_2, χ_3 are expressed as a function of ψ_1, ψ_2, ψ_3 (eq. (14) of paper-2) :

$$\chi_1 = \frac{1}{\sqrt{6(1-S)}} (-\psi_1 - \psi_2 + 2\psi_3)$$

$$\chi_2 = \frac{1}{\sqrt{2(1-S)}} (\psi_1 - \psi_2) \quad (11)$$

$$\chi_3 = \frac{1}{\sqrt{3(1+2S)}} (\psi_1 + \psi_2 + \psi_3)$$

S being the overlap integral between the ψ functions.

The ψ_1, ψ_2, ψ_3 wavefunctions, defined in paper-2, represent the relaxed states in the three potential wells respectively, when a Jahn-Teller coupling with E -modes occurs :

$$\psi_1 = \left[\alpha \left(-\frac{1}{2} E_- + \frac{\sqrt{3}}{2} E_+ \right) + \beta A_2 \right] \varphi'_1$$

$$\psi_2 = \left[\alpha \left(-\frac{1}{2} E_- - \frac{\sqrt{3}}{2} E_+ \right) + \beta A_2 \right] \varphi'_2 \quad (12)$$

$$\psi_3 = (\alpha E_- + \beta A_2) \varphi'_3 .$$

The vibrational wave functions $\varphi'_1, \varphi'_2, \varphi'_3$ and the values of α and β depend upon the E -modes operating in the Jahn-Teller effect.

In this model the experimental parameters b'', a'', μ, ν satisfy the following equations :

$$\frac{b''}{a''} = \frac{b_e [(\alpha^2 + 2\sqrt{2}\alpha\beta) + 2\gamma(\alpha^2 - \sqrt{2}\alpha\beta)] + b_t \left[(\alpha^2 - \sqrt{2}\alpha\beta) + 2\gamma \left(\alpha^2 + \frac{\alpha\beta}{\sqrt{2}} \right) \right]}{\frac{b_e}{\sqrt{2}} [(\alpha^2 + 2\sqrt{2}\alpha\beta) + 2\gamma(\alpha^2 - \sqrt{2}\alpha\beta)] - \frac{b_t}{2\sqrt{2}} \left[(\alpha^2 - \sqrt{2}\alpha\beta) + 2\gamma \left(\alpha^2 + \frac{\alpha\beta}{\sqrt{2}} \right) \right]}$$

$$\mu = \frac{b_e [(\alpha^2 + 2\sqrt{2}\alpha\beta) - \gamma(\alpha^2 - \sqrt{2}\alpha\beta)] + b_t \left[(\alpha^2 - \sqrt{2}\alpha\beta) - \gamma \left(\alpha^2 + \frac{\alpha\beta}{\sqrt{2}} \right) \right]}{b_e [(\alpha^2 + 2\sqrt{2}\alpha\beta) + 2\gamma(\alpha^2 - \sqrt{2}\alpha\beta)] + b_t \left[(\alpha^2 - \sqrt{2}\alpha\beta) + 2\gamma \left(\alpha^2 + \frac{\alpha\beta}{\sqrt{2}} \right) \right]} \quad (13)$$

$$\nu = \frac{b_e [(\alpha^2 + 2\sqrt{2}\alpha\beta) - \gamma(\alpha^2 - \sqrt{2}\alpha\beta)] - \frac{b_t}{2} \left[(\alpha^2 - \sqrt{2}\alpha\beta) - \gamma \left(\alpha^2 + \frac{\alpha\beta}{\sqrt{2}} \right) \right]}{b_e [(\alpha^2 + 2\sqrt{2}\alpha\beta) + 2\gamma(\alpha^2 - \sqrt{2}\alpha\beta)] - \frac{b_t}{2} \left[(\alpha^2 - \sqrt{2}\alpha\beta) + 2\gamma \left(\alpha^2 + \frac{\alpha\beta}{\sqrt{2}} \right) \right]}$$

where γ is the overlap integral between the vibrational functions $\varphi'_1, \varphi'_2, \varphi'_3$.

b_e measures the interaction of electrons with tetragonal strains and b_t with trigonal strains. These two constants are defined in eq. (21) of paper-1.

We have three equations which allow us to calculate the three unknown quantities $b_e/b_t, \alpha/\beta$ and γ . Furthermore, the normal coordinates of modes responsible of the Jahn-Teller effect are (see paper-3) :

$$Q_+^0 = AQ_3 + BQ'_6 \quad \text{or} \quad Q_-^0 = AQ_2 + BQ'_5$$

Q_3 and Q_2 , the normal coordinates of tetragonal E -modes ;

Q'_6 and Q'_5 , the normal coordinates of trigonal E -modes.

The electronic wave function $\alpha E_- + \beta A_2$ for the minimum lying on the Q_+^0 direction, is determined by diagonalizing the following matrix, in the A_2, E_- representation (paper-3) :

$$\begin{pmatrix} 2\delta & -\sqrt{2}AV_e\rho' + \frac{B}{\sqrt{2}}V_t\rho' \\ -\sqrt{2}AV_e\rho' + \frac{B}{\sqrt{2}}V_t\rho' & -\delta - AV_e\rho' - BV_t\rho' \end{pmatrix}. \quad (14)$$

The cubic approximation is used for the electronic system :

$$V_e = -\langle E_- | \mathcal{U}_x^e | E_- \rangle = -\frac{1}{\sqrt{2}}\langle E_- | \mathcal{U}_x^e | A_2 \rangle$$

$$V_t = -\langle E_- | \mathcal{U}_x^t | E_- \rangle = \sqrt{2}\langle E_- | \mathcal{U}_x^t | A_2 \rangle$$

ρ' is defined as in the paper-3 (eq. (19)) :

$$\rho' = \langle \varphi'_3 | Q_+^0 | \varphi'_3 \rangle.$$

In our model we have (eq. (21) of paper-3)

$$V_e = -\frac{\sqrt{3}}{4} \frac{b_e}{R} \quad \text{and} \quad V_t = \frac{\sqrt{3}}{4\sqrt{2}} \frac{b_t}{R} \quad (15)$$

where R is the cation-anion distance.

With the values of b_e/b_t and β/α given by the eq. (13) we are able to calculate the ratio A/B with the matrix (14) and the eq. (15), knowing that the Jahn-Teller coupling is not very strong.

The negative values of b''/a'' give more coherent results than positive values. With $b''/a'' \simeq -2.6$, $\mu \simeq 0.71$, $\nu \simeq 0.66$, we obtain reasonable results : $b_e/b_t \simeq 0.06$, $\beta/\alpha \simeq 0.25$ and $\gamma \simeq 0.2$. Choosing $V_t\rho'$ approximately equal to 4δ , with these values of b_e/b_t and β/α we deduce that $A/B \simeq 1$. The value of A/B strongly depends on the experimental values of b''/a'' , μ and ν . However this calculation shows that the modes responsible for the Jahn-Teller effect are not purely tetragonal. The contribution of the trigonal coordinates (Q'_5, Q'_6) in the normal coordinates of these modes is certainly large.

These results agree with the conclusions obtained for the Cr^{3+} ion [3]. The sign of the ratio b''/a'' for Co^{3+} must be experimentally the same as this of b''/a'' for Cr^{3+} . Now we have shown that the negative sign of b''/a'' for Cr^{3+} is more likely, and consequently the normal coordinates of the vibration modes

responsible of the Jahn-Teller effect would be a mixing of tetragonal and trigonal coordinates, the trigonal contribution being the largest [3]. Similar conclusions have been obtained for V^{3+} [7].

The 61.5 cm^{-1} splitting between the χ_3 and χ_1, χ_2 levels for a zero pressure is not only due to the trigonal splitting quenched by the γ factor. It is also due to the tunnelling between the three potential wells because the vibronic functions ψ_1, ψ_2, ψ_3 are not orthogonal. The problem is like this one of a Jahn-Teller effect for a doublet state in cubic symmetry with warping [8, 9].

5. Conclusion. — The effect of a stress on the ${}^1A_1 \rightarrow {}^1T_1$ transition of Co^{3+} in $\alpha\text{-Al}_2\text{O}_3$ is well interpreted by a phenomenological matrix, based on the group theory. From the experimental parameters we have calculated the relative values of the local elastic compliances such as $S_{11}^* - S_{12}^*, S_{44}^*, S_{14}^*, S_{15}^*$. These values show that the local deformation obeys the C_3 ($\sim C_{3v}$) local symmetry rather than the D_{3d} crystal symmetry, as in the case of Cr^{3+} . The relative value of S_{15}^* is very large.

The splitting between the non degenerate χ_3 level and the degenerate χ_1, χ_2 level for a zero pressure show that the Jahn-Teller effect is not strong. The negative sign of b''/a'' (~ -2.6) seems more likely, and the normal coordinates of the vibration modes responsible of the Jahn-Teller effect would be a linear combination of tetragonal (Q_2, Q_3) and trigonal coordinates (Q'_5, Q'_6). These conclusions agree with these obtained for Cr^{3+} and V^{3+} ions [3, 7].

APPENDIX

Matrices of the strain hamiltonian \mathcal{H}_d in χ_3, χ_2, χ_1 basis. — 1. For a pressure applied along an axis perpendicular or parallel to a C_2 -axis and perpendicular to the C_3 -axis. — The lower sign is for p parallel to the C_2 -axis and the upper sign for p perpendicular to the C_2 -axis. The 3 B splitting is equal to the splitting between the non degenerate state χ_3 and twice-degenerate states χ_1, χ_2 , for the free crystal, plus the splitting proceeding of the $\frac{2}{6} \frac{\varepsilon_{zz}^* - \varepsilon_{xx}^* - \varepsilon_{yy}^*}{6}$ deformation when a pressure equal to p is applied.

$$p \begin{pmatrix} \chi_3 & \chi_2 & \chi_1 \\ 2B/p & \mp \frac{1}{2\sqrt{2}} va'' S_{14}^* & \pm \mu \frac{b''}{4\sqrt{2}} (S_{11}^* - S_{12}^*) \pm \frac{va''}{2\sqrt{2}} S_{15}^* \\ \mp \frac{1}{2\sqrt{2}} va'' S_{14}^* & -\frac{B}{p} \mp \frac{b''}{8} (S_{11}^* - S_{12}^*) \mp \frac{a''}{4} S_{15}^* & \pm \frac{a''}{4} S_{14}^* \\ \pm \mu \frac{b''}{4\sqrt{2}} (S_{11}^* - S_{12}^*) \pm \frac{va''}{2\sqrt{2}} S_{15}^* & \pm \frac{a''}{4} S_{14}^* & -\frac{B}{p} \pm \frac{b''}{8} (S_{11}^* - S_{12}^*) \pm \frac{a''}{4} S_{15}^* \end{pmatrix} \quad (A 1)$$

2. For a pressure applied along an axis whose direction cosines are $k \neq 0, l = 0, m \neq 0$.

$$p \begin{pmatrix} \chi_3 & \chi_2 & \chi_1 \\ 2B/p & \frac{k^2}{2\sqrt{2}} va'' S_{14}^* \mp \frac{km}{2\sqrt{2}} \mu b'' S_{14}^* & -\frac{\mu b''}{4\sqrt{2}} [k^2(S_{11}^* - S_{12}^*) \mp 2 km S_{15}^*] - \\ & & -\frac{k^2}{2\sqrt{2}} va'' S_{15}^* \mp \frac{km}{2\sqrt{2}} va'' S_{44}^* \\ \frac{k^2}{2\sqrt{2}} va'' S_{14}^* \mp \frac{km}{2\sqrt{2}} \mu b'' S_{14}^* & -\frac{B}{p} + \frac{b''}{8} [k^2(S_{11}^* - S_{12}^*) \pm 2 km S_{15}^*] + \\ & & + \frac{k^2 a'' S_{15}^*}{4} \pm \frac{km}{4} a'' S_{44}^* \\ -\frac{\mu b''}{4\sqrt{2}} [k^2(S_{11}^* - S_{12}^*) \mp 2 km S_{15}^*] - \\ & & -\frac{k^2 a'' S_{14}^*}{4} \pm \frac{km}{4} b'' S_{14}^* \\ -\frac{k^2}{2\sqrt{2}} va'' S_{15}^* \mp \frac{km}{2\sqrt{2}} va'' S_{44}^* & & -\frac{B}{p} - \frac{b''}{8} [k^2(S_{11}^* - S_{12}^*) \pm 2 km S_{15}^*] - \\ & & -\frac{k^2 a'' S_{15}^*}{4} \mp \frac{km}{4} a'' S_{44}^* \end{pmatrix} \quad (A 2)$$

The upper sign is for the sites of type I or II and the lower sign for the sites of type III or IV.

3. For a pressure applied along an axis whose direction cosines are $k = 0, l \neq 0, m \neq 0$.

$$p \begin{pmatrix} \chi_3 & \chi_2 & \chi_1 \\ 2B/p & -\frac{l^2 va'' S_{14}^*}{2\sqrt{2}} + \frac{mva'' S_{44}^*}{2\sqrt{2}} + \\ & & + \frac{lm}{2\sqrt{2}} \mu b'' S_{15}^* & \frac{\mu b''}{4\sqrt{2}} [l^2(S_{11}^* - S_{12}^*) - 2 lm S_{14}^*] + \\ & & & + \frac{l^2 va''}{2\sqrt{2}} S_{15}^* \\ -\frac{l^2 va'' S_{14}^*}{2\sqrt{2}} + \frac{mva'' S_{44}^*}{2\sqrt{2}} + \\ & & + \frac{lm}{2\sqrt{2}} b'' S_{15}^* & -\frac{B}{p} - \frac{b''}{8} [l^2(S_{11}^* - S_{12}^*) - 2 lm S_{14}^*] - \\ & & - \frac{l^2 a'' S_{15}^*}{4} & \frac{l^2 a'' S_{14}^*}{4} - \frac{lma'' S_{44}^*}{4} - \frac{lm}{4} b'' S_{15}^* \\ \frac{\mu b''}{4\sqrt{2}} [l^2(S_{11}^* - S_{12}^*) - 2 lm S_{14}^*] + \\ & & + \frac{l^2 va''}{2\sqrt{2}} S_{15}^* & -\frac{B}{p} + \frac{b''}{8} [l^2(S_{11}^* - S_{12}^*) - 2 lm S_{14}^*] + \\ & & & + \frac{l^2 a'' S_{15}^*}{4} \end{pmatrix} \quad (A 3)$$

References

- [1] LACROIX, R., DUVAL, E., CHAMPAGNON, B., LOUAT, R., *Phys. Stat. Sol.* **68B** (1975) 473.
- [2] DUVAL, E., LOUAT, R., LACROIX, R., *Phys. Stat. Sol.* **50** (1972) 627.
- [3] LOUAT, R., LACROIX, R., DUVAL, E., CHAMPAGNON, B., *Phys. Stat. Sol.* **68B** (1975).
- [4] JASPERSON, S. N. and SCHNATTERLY, S. E., *Rev. Sci. Instrum.* **40** (1969) 761.
- [5] MC CLURE, D. S., *J. Chem. Phys.* **36** (1962) 2757.
- [6] HENRY, C. H., SCHNATTERLY, S. E. and SLICHTER, C. P., *Phys. Rev.* **137** (1965) 583.
- [7] CHAMPAGNON, B., DUVAL, E., LOUAT, R., *Phys. Stat. Sol.* **69B** (1975).
- [8] O'BRIEN, M. C. M., *Proc. R. Soc. A* **281** (1964) 323.
- [9] HAM, F. S., *Electron Paramagnetic resonance*, Ed. S. Geschwind (N. Y. Plenum Press) 1971.
-